Renewable Energy 36 (2011) 1754–1760

Contents lists available at ScienceDirect

Renewable Energy

journal homepage: www.elsevier.com/locate/renene

Quaternion-valued short-term joint forecasting of three-dimensional wind and atmospheric parameters

C. Cheong Took [a,*], G. Strbac [a], K. Aihara [b], D.P. Mandic [a]

[a] Department of Electrical and Electronic Engineering, Imperial College London, London SW7 2AZ, United Kingdom
[b] FIRST, Aihara Innovative Mathematical Modelling Project (Japan Society for Promotion of Science) and University of Tokyo, Japan

ARTICLE INFO

Article history:
Received 17 July 2010
Accepted 13 December 2010
Available online 8 January 2011

Keywords:
Wind forecasting
Quaternion-valued representation
Augmented quaternion statistics
Widely linear quaternion least mean square (WL-QLMS)
Fusion of atmospheric parameters
Data fusion via vector spaces

ABSTRACT

This work introduces novel methodology for the simultaneous modelling and forecasting of three-dimensional wind field. This is achieved based on a quaternion wind model, which by virtue of its division algebra accounts naturally for the coupling between the three wind dimensions. To fully exploit the available second order statistics, we employ the newly developed augmented quaternion statistics and perform prediction based on the widely linear model. The proposed quaternion domain processing also facilitates the fusion of external atmospheric parameters, such as air temperature, yielding improved forecasts. Simulations for wind regimes with different dynamics and over a range of prediction horizons, together with the fusion of air temperature, support the approach.

1. Introduction

There has been a growing interest in so-called 'green' energy sources and, for example, wind farm technology is becoming an integral part of the electricity grid [1,21]. One important component of this technology is the use of control engineering, such as in the mitigation of wind forced vibrations on wind turbines [2,3]. To address the problems arising from intermittency associated with the wind as an energy source, prediction based control in this context can assist in:

1. monitoring and controlling the vibrations of the wind turbine in real time, hence providing more accurate and robust damage protection;
2. automatic optimisation of wind turbine (WT) parameters, such as the adjustment of the rotor blade to the correct elevation angle, maximising the area of the rotor exposed to the wind [4];
3. smoothing out the variation in wind power production with battery storage to ensure the scheduling plan is enforced, thus improving market operation [5];
4. enhancing power management over a network of WTs through the forecasting of the power generation via wind prediction. This also facilitates the integration of the so-called 'smart grid' technologies [6].

Short-term wind forecasting plays a key role in the wind farm control technology [4,5,7,9,10]; the distinctive feature of our approach is that it is based on the assumption that both the wind speed and direction influence the power output. For example, milder winds generally come from a wide range of angles (directions) [12], making the estimation of wind direction a non-negligible factor in the intelligent operation of a WT. The importance of wind direction in this context is particularly significant in spatial correlation studies used, for example, to determine the position of WT in a wind park.

Wind speed is directly related to the power output P of the WT, according to [13,14]

$$P = \frac{1}{2}\rho C A v^3 \tag{1}$$

where ρ denotes air density, A the area swept by the rotor, v the wind speed component perpendicular to the area swept by the rotor and C the power coefficient. In two-dimensional (2D) wind forecasting, recent studies have successfully employed simultaneous modelling of both the wind speed and direction by virtue of complex domain processing [8–10]. Such complex domain modelling was performed

* Corresponding author. Tel.: +44 7515436519; fax: +44 207594 6302.
E-mail addresses: c.cheong-took@imperial.ac.uk (C.C. Took), g.strbac@imperial.ac.uk (G. Strbac), aihara@sat.t.u-tokyo.ac.jp (K. Aihara), d.mandic@imperial.ac.uk (D.P. Mandic).

0960-1481/$ – see front matter © 2010 Elsevier Ltd. All rights reserved.
doi:10.1016/j.renene.2010.12.013

both based on standard complex models [7,9] and those based on the so-called 'augmented complex statistics', accounting for the likely rotational dependence of signal distributions, as shown in Fig. 1. Whereas the complex model is proven suitable for the forecasting related to optimisation of power output, modern anemometers also measure the vertical wind speed (or equivalently the speed vector and spherical angle) and some atmospheric parameters (air temperature, air density). These parameters are very important in the modelling of the vibrations of wind turbines and in protection against damage due to sudden gusts and turbulent air [2,3,27,28]. It is therefore likely that the estimation of wind speed and direction based on a quaternion model, which accounts naturally for the 3D wind speed and atmospheric parameters, will be more accurate than that based on complex 2D model, both in the 2D estimation and in cases where a combination of 2D models is not sufficient to model 3D and 4D phenomena.

In this work, we aim to investigate whether our existing 2D wind forecasting algorithms [5,7,10] can be extended to four-dimensional (4D) models, and thus cater for all the three wind speed components and air temperature.

In connection with power output, wind speed recorded from the Vertical (V) direction, along with the resultant speed from the North–South (N–S) and East–West (E–W) direction determines the optimal angle of attack (aerodynamic parameter) between the blade and the incoming free-stream wind [14]. Based on this optimal angle of attack, the blade pitch angle (design parameter) can then be tuned accordingly to maximise the power coefficient C in (1). As for air temperature, it affects the output power P in (1) in the following ways:

- The air density ρ is governed by air temperature T since $\rho = P/(RT)$, where P, R, T denote the absolute pressure (Pascal), the specific gas constant (Joules per Kilogramme per Kelvin), and the absolute temperature (Kelvin). Although, it is common to assume $\rho = 1.225$, a 3% error in air density leads to a 3% error in the power output (1). In the context of a network of WTs, the error accumulated from each WT is not negligible in the management of power grid.
- Existing studies suggest a strong correlation between air temperature and wind speeds [15,16], as confirmed in our statistical analysis of the wind data and in simulation studies. As wind speed is the most prominent factor in power output estimation (see equation (1)), we aim to exploit this correlation to improve the prediction of wind speeds in order to maximise the power output.

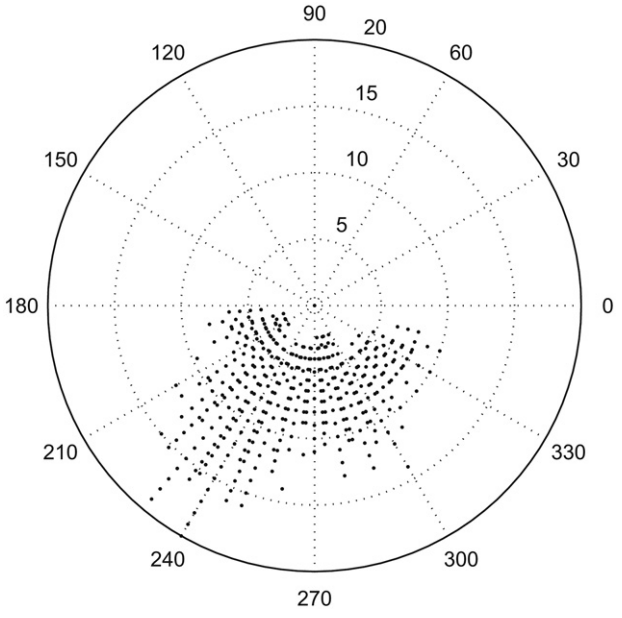

Fig. 1. Wind lattice (angular distribution of wind speed).

One convenient way to represent wind field is to consider simultaneously the three perpendicular wind speeds and temperature as a full quaternion-valued quantity, a hypercomplex extension of the two-dimensional complex-valued wind model [9,10], given by

$$q = \tau + \imath\nu_E + \jmath\nu_N + \kappa\nu_V \tag{2}$$

where ν_E, ν_N, ν_V and τ denote respectively the wind speeds measured in the East–West direction, North–South direction, Vertical direction (metres per second), and the temperature (Celsius). Observe that the relationship between the three imaginary components $\imath$, $\jmath$, κ of a quaternion is given by [11]

$$\begin{aligned} &\imath\jmath = \kappa \quad \jmath\kappa = \imath \quad \kappa\imath = \jmath \\ &\imath\jmath\kappa = \imath^2 = \jmath^2 = \kappa^2 = -1 \end{aligned} \tag{3}$$

If the air temperature is not a part of the hypercomplex wind field model (2), then we have the so-called "pure quaternion" $q = \imath\nu_E + \jmath\nu_N + \kappa\nu_V$, which models 3D wind speed only, as illustrated in Fig. 2. Notice that by using quaternions, both the full and pure quaternion models account naturally for the statistical dependence between the wind measurements (such as wind speeds and air temperature); this is instrumental in avoiding the undermodelling errors introduced by standard dual univariate models [17] or the corresponding quadruple univariate real-valued models. The quaternion domain modelling also allows for the use of new developments in quaternion statistics - so-called augmented statistics, to take advantage of the noncircular distributions and nonstationarity of the intermittent wind signals [18], as discussed in Section 3. This way, we can exploit the time-varying correlation between each dimension of the signal, and improve prediction accuracy. Prior to the formulation of the proposed forecasting framework, we shall investigate statistical properties of the wind data, followed by details of quaternion statistics in Section 3.

2. Wind characteristics

Two anemometers were used to record the wind data[1] at a sampling frequency of 32 Hz; the first anemometer (labelled as "North") was positioned in the North direction, and the second anemometer (labelled as "South") was placed 5 m south of the "North" anemometer. Table 1 shows the interchannel correlation properties of these wind data, calculated based on Pearson's coefficient

$$\rho_{xy} = \frac{E\{x-\overline{x}\}E\{y-\overline{y}\}}{\sigma_x\sigma_y} \tag{4}$$

where $E\{\cdot\}$ is the statistical expectation operator, $\overline{(\cdot)}$ the mean value operator, σ standard deviation, and $-1 \le \rho_{xy} \le 1$. Notice that $\rho_{xy} = 1$ indicates a perfect positive linear relationship, and conversely $\rho_{xy} = -1$ indicates perfect negative linear relationship between x and y. The wind measurements pertaining to the North anemometer are denoted as $\{\tau_1,\nu_{E1},\nu_{N1},\nu_{V1}\}$ and similarly for the South anemometer measurements $\{\tau_2,\nu_{E2},\nu_{N2},\nu_{V2}\}$, and are incorporated in the quaternion model (2).

[1] The measurements were conducted by Aihara Laboratory, in urban environment, at the Institute for Industrial Science, University of Tokyo, Japan.

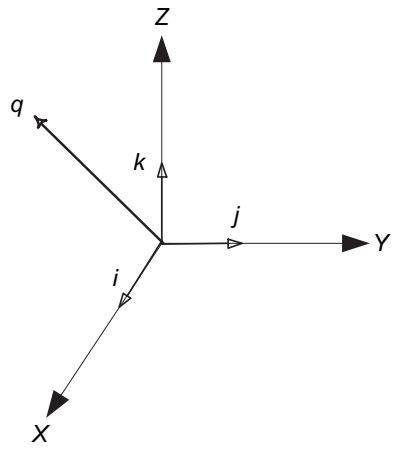

Fig. 2. A three-dimensional wind vector as a pure quaternion q.

Table 2 summarises the statistical properties of the two datasets considered. Observe that the last feature $\sum|\rho_{xy}|$ indicates the cross-correlation of a particular wind measurement with other wind measurements. For instance, the cross-correlation of the wind speed E_1 is the sum of the absolute value of the entries of the first column of Table 1, except for the first entry. Symbols N, σ_x, $\bar{x}$, min, max denote respectively the number of samples, standard deviation, the mean value, minimum and maximum values.

2.1. Discussion

From Table 1, it is clear that the highest degree of correlation came from the East–West wind speeds and the air temperatures, conforming with the studies in Refs. [15,16]; the strong correlation between wind speed and air temperature also justifies our quaternionic forecasting framework. Table 2 (via the standard deviation σ) indicates that the wind blowing from the North–South direction was the strongest source of energy, whereas the Vertical direction was the weakest source of energy; this is also reflected in the behaviour of the $\sum|\rho_{xy}|$ coefficient. We shall now proceed to demonstrate how these couplings can be exploited conveniently for enhanced wind forecasting in the quaternion domain $\mathbb{H}$.

3. Augmented quaternion statistics

Consider four centred real-valued random vectors $\mathbf{q}_a$,$\mathbf{q}_b$,$\mathbf{q}_c$,$\mathbf{q}_d$; complete statistics of these variables are given by 10 real-valued covariance matrices

Table 1
Correlation properties of the 4D wind datasets, with ν denoting wind speeds in the three perpendicular directions, and τ air temperature.

	North				South			
	ν_{E1}	ν_{N1}	ν_{V1}	τ_1	ν_{E2}	ν_{N2}	ν_{V2}	τ_2
ν_{E1}	1.00	0.32	−0.04	0.55	0.53	0.07	0.10	0.64
ν_{N1}	0.32	1.00	−0.08	0.08	−0.01	0.65	0.02	0.12
ν_{V1}	−0.04	−0.08	1.00	0.18	0.04	−0.21	0.08	0.02
τ_1	0.55	0.08	0.18	1.00	0.30	−0.15	0.10	0.44
ν_{E2}	0.53	−0.01	0.04	0.30	1.00	−0.08	0.22	0.65
ν_{N2}	0.07	0.65	−0.21	−0.15	−0.08	1.00	−0.16	−0.12
ν_{V2}	0.10	−0.02	0.08	0.10	0.22	−0.16	1.00	0.19
τ_2	0.64	0.12	0.02	0.44	0.65	−0.12	0.19	1.00

$$\begin{aligned} C_{\mathbf{q}_i} &= E\{\mathbf{q}_i\mathbf{q}_i\} \quad i\forall\{a,b,c,d\} \\ C_{\mathbf{q}_a\mathbf{q}_b} &= E\{\mathbf{q}_a\mathbf{q}_b\} \quad C_{\mathbf{q}_a\mathbf{q}_c} = E\{\mathbf{q}_a\mathbf{q}_c\} \\ C_{\mathbf{q}_a\mathbf{q}_d} &= E\{\mathbf{q}_a\mathbf{q}_d\} \quad C_{\mathbf{q}_c\mathbf{q}_d} = E\{\mathbf{q}_c\mathbf{q}_d\} \\ C_{\mathbf{q}_b\mathbf{q}_c} &= E\{\mathbf{q}_b\mathbf{q}_c\} \quad C_{\mathbf{q}_b\mathbf{q}_d} = E\{\mathbf{q}_b\mathbf{q}_d\} \end{aligned} \tag{5}$$

These real-valued matrices have an equivalent compact representation in the quaternion domain $\mathbb{H}$, given by

$$\begin{aligned} C_{\mathbf{q}} &= E\{\mathbf{q}\mathbf{q}^H\} \quad C_{\mathbf{q}}^{\imath} = E\{\mathbf{q}\mathbf{q}^{\imath H}\} \\ C_{\mathbf{q}}^{\jmath} &= E\{\mathbf{q}\mathbf{q}^{\jmath H}\} \quad C_{\mathbf{q}}^{\kappa} = E\{\mathbf{q}\mathbf{q}^{\kappa H}\} \end{aligned} \tag{6}$$

where $(\cdot)^H$ denotes the Hermitian transpose, $\mathbf{q} = \mathbf{q}_a + \imath\mathbf{q}_b + \jmath\mathbf{q}_c + \kappa\mathbf{q}_d$, and the so-called quaternion involutions $\mathbf{q}^{\imath}$, $\mathbf{q}^{\jmath}$, $\mathbf{q}^{\kappa}$ are defined as

$$\begin{aligned} \mathbf{q}^{\imath} &= \mathbf{q}_a + \imath\mathbf{q}_b - \jmath\mathbf{q}_c - \kappa\mathbf{q}_d \\ \mathbf{q}^{\jmath} &= \mathbf{q}_a - \imath\mathbf{q}_b + \jmath\mathbf{q}_c - \kappa\mathbf{q}_d \\ \mathbf{q}^{\kappa} &= \mathbf{q}_a - \imath\mathbf{q}_b - \jmath\mathbf{q}_c + \kappa\mathbf{q}_d \end{aligned} \tag{7}$$

Observe that these quaternion involutions are similar to the conjugate operation $(\cdot)^*$ in the complex domain, in the sense that they are self inverse componentwise mappings. We can solve Eq. (6) to derive the corresponding real-valued quadrivariate statistics in (5), for example,

$$C_{\mathbf{q}_a} = \frac{1}{4}\Re\left\{C_{\mathbf{q}} + C_{\mathbf{q}}^{\imath} + C_{\mathbf{q}}^{\jmath} + C_{\mathbf{q}}^{\kappa}\right\}$$

where $\Re\{\cdot\}$ denotes the real part of a quaternion vector; for more details on advanced quaternion statistics, see Ref. [18]. In the context of our four-dimensional wind model, the quadrivariate nature of the quaternion domain $\mathbb{H}$ makes it a natural choice to perform wind forecasting and to simplify the computation by reducing the 10 real-valued covariance matrices in (5) to only four quaternion-valued covariance matrices in (6). This results in an ease of implementation, while still exploiting the full second order statistical information from the quaternion-valued representation of the wind.

4. The forecasting configuration

Due to the intermittent and nonstationary nature of wind, we need to employ an adaptive prediction setting whereby at time instant k, the prediction algorithm estimates the wind vector $(k+T)$ steps ahead, based on the present and past samples at k,…,$(k-N+1)$ [24,26]. This is achieved by employing the quaternion widely linear adaptive filter [20], which makes use of the augmented quaternion statistics [18]. We also demonstrate how to predict simultaneously heterogeneous wind parameters [22,23] such as wind direction and 3D wind speed, used for the intelligent manipulation of the blades of the wind turbine with respect to the angle of attack of the wind.

4.1. The adaptive prediction algorithm WL-QLMS

To account for the complete second order statistics in (6), we need to consider not only the quaternion variable $\mathbf{q}$, but also its involutions $\mathbf{q}^{\imath}$, $\mathbf{q}^{\jmath}$, $\mathbf{q}^{\kappa}$. Therefore, the predicted estimate y of the adaptive widely linear quaternion least mean square (WL-QLMS) algorithm can be expressed in terms of the past samples of the wind $\mathbf{q} = [q(k),\ldots,q(k-N-1)]^T$ as

$$y = \mathbf{w}^{aH}\mathbf{q}^a = \mathbf{g}^H\mathbf{q} + \mathbf{h}^H\mathbf{q}^{\imath} + \mathbf{u}^H\mathbf{q}^{\jmath} + \mathbf{v}^H\mathbf{q}^{\kappa} \tag{8}$$

where the augmented tap input vector $\mathbf{q}^a$ and its corresponding adaptive weight coefficients $\mathbf{w}^a$ are given by

Table 2
Statistical properties of the wind datasets.

	North				South			
	E_1	N_1	V_1	T_1	E_2	N_2	V_2	T_2
N	6000	6000	6000	6000	6000	6000	6000	6000
σ_x	0.29	0.39	0.16	0.13	0.25	0.36	0.13	0.14
$\bar{x}$	−0.22	0.22	−0.09	31.19	−0.29	0.11	0.01	29.44
min	−1.21	−0.90	−0.62	30.97	−1.14	−0.64	−0.47	29.18
max	0.44	1.53	0.53	31.66	0.28	1.31	0.45	29.90
$\sum \lvert\rho_{xy}\rvert$	2.25	1.28	0.65	1.8	1.83	1.44	0.87	2.18

$$\mathbf{w}^a = [g_1(k),\ldots,g_N(k),h_1(k),\ldots,h_N(k),u_1(k),\ldots,u_N(k), v_1(k),\ldots,v_N(k)]^T$$

$$\mathbf{q}^a = [q(k),\ldots,q(k-N-1),q^i(k),\ldots,q^i(k-N-1), q^j(k),\ldots,q^j(k-N-1),q^\kappa(k),\ldots,q^\kappa(k-N-1)]^T$$

and the symbol $(\cdot)^T$ denotes the vector transpose operator. The error signal $e(k)$ required for the adaptation of the adaptive weights is obtained from

$$e(k) = d(k) - y(k) = e_a(k) + \imath e_b(k) + \jmath e_c(k) + \kappa e_d(k) \tag{9}$$

and is employed in the quadratic cost function $\mathcal{J}(k)$, corresponding to the error power defined by

$$\mathcal{J}(k) = |e(n)|^2 = e(k)e^*(k) \tag{10}$$

The cost function (10) is minimised recursively by

$$\mathbf{w}^a(k+1) = \mathbf{w}^a(k) - \mu\frac{\partial\mathcal{J}(k)}{\partial\mathbf{w}^a(k)} \tag{11}$$

where μ is the rate of adaptation, and the gradient with respect to the augmented adaptive weight vector $\mathbf{w}_a$ is given by (for more detail on the derivation see Refs. [19,20])

$$\frac{\partial\mathcal{J}(k)}{\partial\mathbf{w}^a(k)} = -\left[2\mathbf{q}^a(k)e^*(k) - e(k)\mathbf{q}^{a*}\right] \tag{12}$$

giving the weight update of WL-QLMS as

$$\mathbf{w}^a(k+1) = \mathbf{w}^a(k) + \mu\left[2\mathbf{q}^a(k)e^*(k) - e(k)\mathbf{q}^{a*}\right] \tag{13}$$

This update is general and caters for both second order circular (proper) signals for which the probability distribution is rotation invariant, and for improper signals. This completes the overview of the quaternion-valued gradient descent based WL-QLMS algorithm.

4.2. The four-dimensional forecasted wind data

As the four-dimensional wind data is forecasted by the WL-QLMS prediction algorithm as

$$y = \mathbf{w}^{aH}\mathbf{q}^a = \widehat{q}(k+T) = \widehat{\tau}(k+T) + \imath\widehat{\nu}_E(k+T) + \jmath\widehat{\nu}_N(k+T) + \kappa\widehat{\nu}_V(k+T)$$

we can cast the predicted $\widehat{q}(k+T)$ 4D wind vector into its horizontal parameters such as wind speed $\widehat{\nu}_{2D}$ and direction $\widehat{\theta}_{2D}$ respectively, as follows [5,10]

$$\begin{aligned}\widehat{\nu}_{2D}(k+T) &= \sqrt{\widehat{\nu}_E^2(k+T) + \widehat{\nu}_N^2(k+T)}\\ \widehat{\theta}_{2D}(k+T) &= \tan^{-1}\left(\frac{\widehat{\nu}_N(k+T)}{\widehat{\nu}_E(k+T)}\right)\end{aligned} \tag{14}$$

These parameters can then be used for the predictive estimation of wind power as described in Ref. [5].

On the other hand, to assist in the intelligent positioning of the blade of the wind turbine with respect to the angle of attack of the wind, we require the forecasting of the three-dimensional (3D) orientation of the wind, which is illustrated in Fig. 3. The 3D orientation of the wind which is governed by spherical coordinates $(|\widehat{\nu}_{3D}|,\widehat{\phi}_{3D},\widehat{\theta}_{3D})$, and can be computed as follows

$$\begin{aligned}|\widehat{\nu}_{3D}(k+T)| &= \sqrt{\widehat{\nu}_E^2(k+T) + \widehat{\nu}_N^2(k+T) + \widehat{\nu}_V^2(k+T)}\\ \widehat{\theta}_{3D}(k+T) &= \cos^{-1}\left(\frac{\widehat{\nu}_V(k+T)}{|\widehat{\nu}_{3D}(k+T)|}\right)\\ \widehat{\Phi}_{3D}(k+T) &= \operatorname{atan2}\left(\widehat{\nu}_N(k+T),\widehat{\nu}_E(k+T)\right)\end{aligned} \tag{15}$$

where atan2$(\cdot)$ is a variant of the function $\tan^{-1}(\cdot)$, that gives the angle from the East–West direction axis to the vector $(\widehat{\nu}_N,\widehat{\nu}_E)$ in the full range $(-\pi,\pi]$. It can conveniently be expressed in terms of $\tan^{-1}(\cdot)$ as

$$\begin{aligned}\operatorname{atan2}\left(\widehat{\nu}_N,\widehat{\nu}_E\right) &= 2\tan^{-1}\left(\frac{\widehat{\nu}_N}{\sqrt{\widehat{\nu}_N^2+\widehat{\nu}_E^2}+\widehat{\nu}_E}\right) \quad \forall\,\widehat{\nu}_N = 0 \quad \widehat{\nu}_E > 0\\ &= 2\tan^{-1}\left(\frac{\sqrt{\widehat{\nu}_N^2+\widehat{\nu}_E^2}-\widehat{\nu}_E}{\widehat{\nu}_N}\right) \quad \forall\,\widehat{\nu}_N \neq 0\\ &= 0 \quad \text{otherwise}\end{aligned}$$

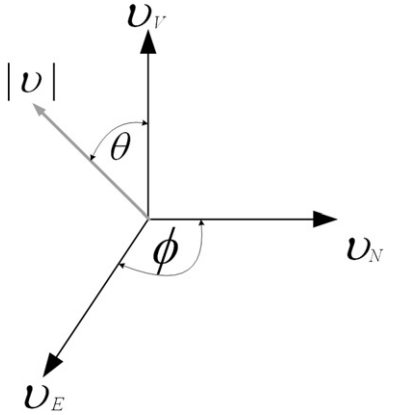

Fig. 3. The three-dimensional orientation model governed by parameters $(|\nu|,\phi,\theta)$, given in Eq. (15).

5. Simulation results and discussion

To evaluate the benefits of the proposed approach, two sets of experiments were conducted on the wind data recorded from the "North" anemometer and a third set on the wind data obtained from "South" anemometer described in Section 2. In the first set of simulations, the 4D quaternion model (2) was assessed against 2D models reported in the literature [5,9,10], whereas in the second experiment we illustrate the advantages of considering the air temperature in wind forecasting. The third set of simulations was performed to test the robustness of the proposed approach.

Performance measure: The measurement used to evaluate the performance was the prediction gain R_p, given by [10,25]

$$R_p = 10\log_{10}\left(\frac{\widehat{\sigma}_q^2}{\widehat{\sigma}_e^2}\right)[\text{dB}] \tag{16}$$

where $\widehat{\sigma}_q^2$ denotes the estimated variance of the input signal $\{q(k)\}$, and $\widehat{\sigma}_e^2$ the estimated variance of the forward prediction error $\{e(k)\}$. For a fair comparison, the power estimates $\widehat{\sigma}_q^2$ and $\widehat{\sigma}_e^2$ were calculated based on the North–South direction and East–West direction in the first and third experiments, whereas in the second experiment $\widehat{\sigma}_q^2$ and $\widehat{\sigma}_e^2$ were estimated by considering all the three perpendicular directions.

5.1. Experiment 1: two-dimensional model versus four-dimensional model

To compare the two-dimensional model with the four-dimensional model on one-step ahead prediction of the horizontal wind speed and direction in (14), we employed the augmented complex least mean square (ACLMS) [10] and the widely linear quaternion least mean square (WL-QLMS) prediction algorithms given in (13), both of which use their respective augmented statistics and widely linear models.

From Fig. 4, it is apparent that the 4D model followed closely the dynamics of both the wind speed and direction, whereas the 2D model followed the general trend of actual wind profile, yielding reasonable but suboptimal estimates (without detail) of both the wind speed and direction. This was confirmed by the prediction gain R_p of 18.66 dB. On the other hand, the additional cross-information from the vertical speed v_v and temperature T of the 4D model significantly improved performance over the 2D model, with a prediction gain of $R_p = 31.46$ dB.

5.2. Experiment 2: three-dimensional model versus four-dimensional model

In Section 2, it was shown that in the datasets considered air temperature had a high degree of correlation with wind speed, as indicated by the high $\sum|\rho_{xy}|$ coefficient in Table 2. The aim of this experiment is to demonstrate the benefit of using air temperature in wind forecasting. This was achieved by assessing the three-dimensional pure quaternion model shown in Fig. 2 of the three perpendicular wind speeds against the four-dimensional full quaternion model in (2) containing air temperature, in a one-step ahead prediction setting.

From Fig. 5, both the 3D and 4D models provided excellent predictions of the wind speeds v_E, v_N, v_V, with the 4D model converging faster, as seen in the right subplot of the wind speed from the North direction. Also, notice that the 4D model followed very closely the highly nonstationary trend of air temperature, yielding improved accuracy over the 3D model, with prediction gain of 33.44 dB against that of 25.94 dB for the 3D model. The corresponding 3D wind speed orientation parameters in Eq. (15), shown in Fig. 6, illustrate visually the advantage of incorporating air temperature in wind forecasting.

5.3. Experiment 3: robustness of the simulation results

To examine robustness of the results obtained in the first two experiments, performances of the adaptive prediction algorithms were evaluated on the set of wind data obtained from the "South" anemometer, as described in Section 2. Furthermore, the prediction

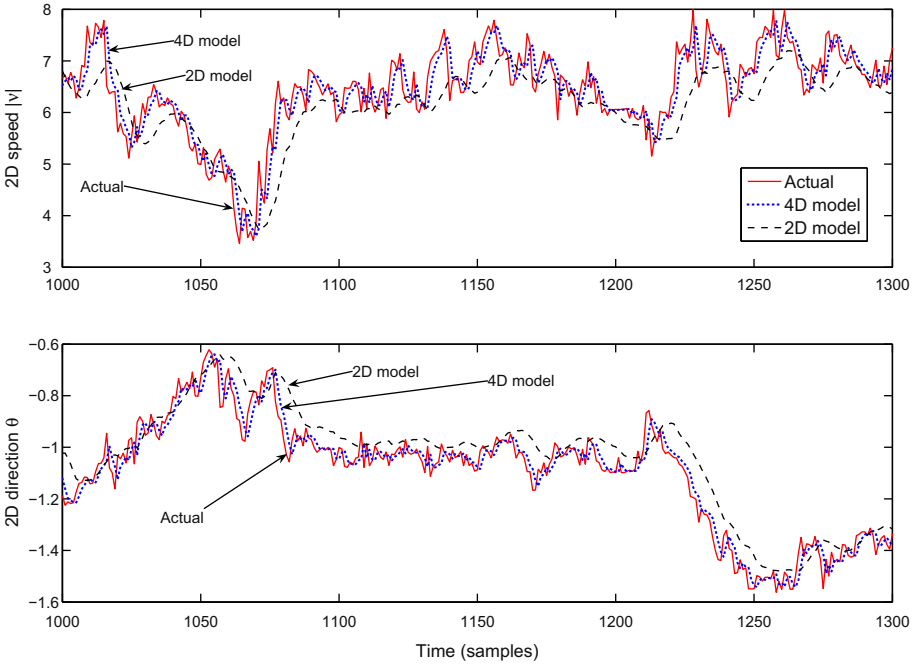

Fig. 4. Performances of the 2D and 4D wind models. Wind speed $|v|$ and direction θ were measured in metres/second and in radians respectively.

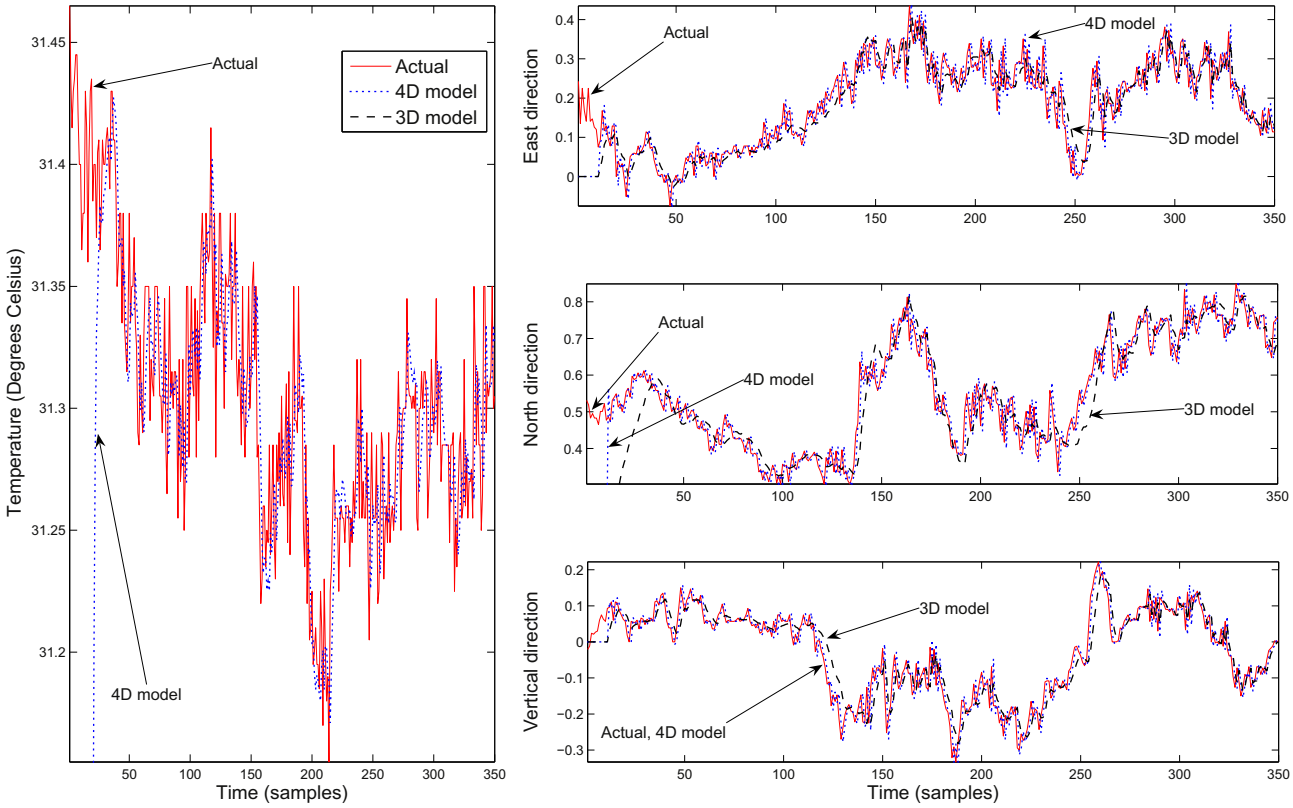

Fig. 5. Performances of the 3D and 4D wind models. Wind speeds in the three perpendicular directions were measured in metres/second.

horizon (in steps ahead) was varied to compare the performances of the 2D, 3D and 4D models. The results are summarised in Table 3.

In all the cases, the increasing length of the prediction horizon caused deterioration in performance, as expected. The 2D (4D) model was the most (least) affected by the size of prediction horizon, confirming that the additional information from the vertical wind speed and air temperature assisted in providing better forecasts. This illustrates the robustness of the results obtained from Experiments 1 and 2, and their consistency with the results of Experiment 3.

6. Concluding remarks

We have introduced a novel methodology for short-term prediction of wind, whereby a quaternion-valued model has been

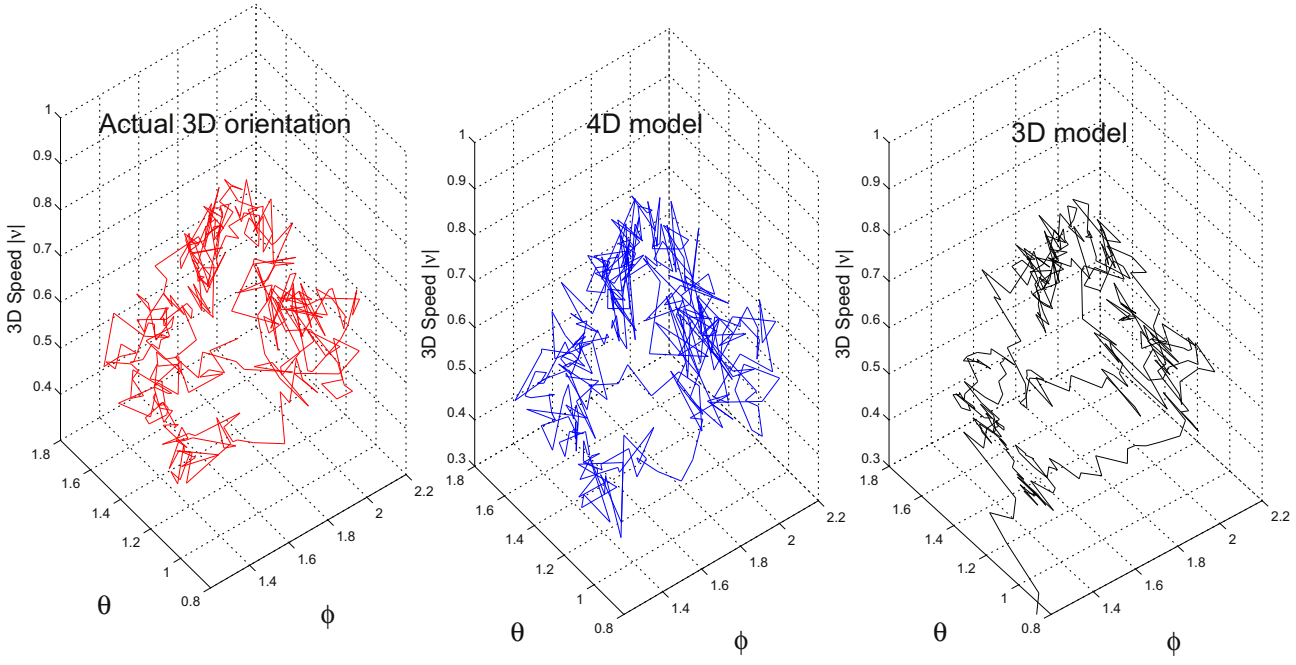

Fig. 6. Orientation of the 3D wind models in Eq. (15). Wind speed $|v|$ was measured in metres/second.

Table 3
Performance measure (16) for varying prediction horizon.

Algorithms	1-Step ahead	10-Steps ahead	20-Steps ahead
2D ACLMS [10]	16.48	15.49	14.32
3D WL-QLMS in Eq. (13)	18.21	17.89	17.04
4D WL-QLMS in Eq. (13)	23.78	23.68	23.60

shown to allow for both the 3D wind modelling (pure quaternion) and the fusion of atmospheric parameters (full quaternion). Recent advances in augmented quaternion statistics have been used to exploit the complete second order information in the forecasting of the wind data (3D wind field and air temperature), which has led to improved prediction accuracies. Simulations on real-world 3D and 4D wind data have illustrated the benefits of the proposed direct multidimensional forecasting approach.

Acknowledgement

We thank Gill instruments for providing us with the 3D WindMaster anemometer, used for the testing of the algorithms. This work was supported by the EPSRC grant EP/H026266/1.

References

[1] Smith JC. Wind power: present realities and future possibilities. Proceedings of the IEEE 2009;97(2):195–7.
[2] Colwella S, Basu B. Tuned liquid column dampers in offshore wind turbines for structural control. Engineering Structures 2009;31(2):358–68.
[3] Murtagh PJ, Ghosh A, Basu B, Broderick BM. Passive control of wind turbine vibrations including blade/tower interaction and rotationally sampled turbulence. Wind Energy 2008;11(4):304–17.
[4] Egedal P, Rubak R, Stiesdal H. Method and apparatus for prediction-based wind turbine control. European Patent Application no 08007394 EP; April 2008.
[5] Khalid M, Savkin AV. A model predictive control approach to the problem of wind power smoothing with controlled battery storage. Renewable Energy 2010;35:1520–6.
[6] Kowahl N, Kuh A. Micro-scale smart grid optimisation. In: Proceedings of IEEE world congress on computational intelligence; 2010. p. 2692–9.
[7] Hirata Y, Mandic DP, Suzuki H, Aihara K. A collaborative approach to the modelling of real world vector fields: predicting the wind direction. Philosophical Transactions of the Royal Society 2008;366:591–607.
[8] Goh SL, Mandic DP. A complex-valued RTRL algorithm for recurrent neural networks. Neural Computation 2004;16(12):2699–713.
[9] Goh SL, Chen M, Popovic DH, Aihara K, Obradovic D, Mandic DP. Complex valued forecasting of wind profile. Renewable Energy 2006;31(11):1733–50.
[10] Mandic DP, Javidi S, Goh SL, Kuh A, Aihara K. Complex-valued prediction of wind profile using augmented complex statistics. Renewable Energy 2009;34(1):196–201.
[11] Ward JP. Quaternions and Cayley numbers: algebra and applications. Kluwer Academic Publisher; 1997.
[12] Li S, Wunsch DC, O'Hair EA, Giesselmann M. Using NNs to estimate wind turbine power generation. IEEE Transaction on Energy Conversion 2001;16(3):276–82.
[13] Manwell JF, McGowan JG, Rogers AL. Wind energy explained: theory, design and application. John Wiley & Sons Inc.; 2002.
[14] Hau E. Wind turbines: fundamentals, technologies, application, economics. 2nd ed. Springer; 2006.
[15] Nkemdirim LC. An empirical relationship between temperature, vapour pressure deficit and wind speed and evaporation during a winter chinook. Theoretical and Applied Climatology 1991;43:123–8.
[16] Perez IA, Garcia MA, Sanchez ML, Torre BD. Fit of wind speed and temperature profiles in the low atmosphere from rass sodar data. Journal of Atmospheric and Solar-Terrestrial Physics 2006;68:1125–35.
[17] Alexiadis MC, Dokopoulos PS, Sahsamanoglou HS, Manousaridis IM. Short term forecasting of wind speed and related electrical power. Solar Energy 1998;63(1):61–8.
[18] Cheong Took C, Mandic D. Augmented second-order statistics of quaternion signals. Signal Processing 2011;91(2):214–24.
[19] Cheong Took C, Mandic DP. The quaternion LMS algorithm for adaptive filtering of hypercomplex processes. IEEE Transactions on Signal Processing 2009;57(4):1316–27.
[20] Cheong Took C, Mandic DP. A quaternion widely linear adaptive filter. IEEE Transactions on Signal Processing 2010;58(8):4427–31.
[21] Mathew S. Wind energy: fundamentals, resource analysis, and economics. Springer; 2006.
[22] Mandic DP, Goh SL, Aihara K. Sequential data fusion via vector spaces: fusion of heterogeneous data in the complex domain. The Journal of VLSI Signal Processing Systems 2007;48:99–108.
[23] Mandic D, Golz M, Kuh A, Obradovic D, Tanaka T, editors. Signal processing techniques for knowledge extraction and information fusion. Springer; 2008.
[24] Wan E. Time series prediction using a neural network with embedded tapped delay-lines. In: Predicting the future and understanding the past, SFI studies in the science of complexity; 1993. p. 195–217.
[25] Haykin S, Li L. Nonlinear adaptive prediction of nonstationary signals. IEEE Transactions on Signal Processing 1995;43(2):526–35.
[26] Drossu R, Obradovic Z. Rapid design of neural networks for time series prediction. IEEE Computational Science and Engineering 1996;3(2):78–89.
[27] Ragwitz M, Kantz. Detecting non-linear structure and predicting turbulent gusts in surface wind velocities. Europhysics Letter 2000;51:595–601.
[28] Kantz H, Holstein D, Ragwitz M, Vitanov NK. Markov chain model for turbulent wind speed data. Physica A 2004;342:315–21.